Original Article
Metformin upregulates the expression of Gli1 in vascular endothelial cells in hyperoxia-exposed neonatal mice

Xiaowen Xiang*, Li Wang*, Lin Zhou, Yanru Chen, Hongping Xia

*Department of Neonatology, Xinhua Hospital, School of Medicine, Shanghai Jiao Tong University, Shanghai 200092, China. *Equal contributors.*

Abstract: Bronchopulmonary dysplasia (BPD) is characterized by arrested alveolar and vascular development in premature infants. Metformin protects against the cardiovascular impairment induced by diabetes. The aim of this study was to investigate whether metformin could also enhance pulmonary vascular development in hyperoxic neonatal mice and investigate possible mechanisms involved. C57BL/6J newborn mice were randomly assigned to either of two groups - the room air group or the hyperoxia group - within 12 h postnatally. The mice were subcutaneously injected with metformin (100 mg/kg) or saline for 14 days. Lung morphology and PECAM-1 (CD31) expression in the lung were evaluated at postnatal days 7 and 14. Ki-67 and Gli1 expression in vascular endothelial cells was evaluated at postnatal day 14 by immunofluorescence staining. Flow cytometry (FCM) was also used to analyze Gli1 expression. Human umbilical vein endothelial cell (HUVECs) were used to investigate the role of metformin in vascular proliferation and tubular formation under 90% oxygen in vitro by cell counting Kti-8 (CCK8) assays and tube formation assays. Exposure to hyperoxia resulted in impaired lung development in newborn mice. Metformin enhanced the terminal airspace and radial alveolar count in newborn mice thus exposed. Immunohistochemistry staining and western blot assays revealed that metformin enhanced the expression of CD31 in hyperoxia-exposed newborn mice. Immunofluorescence staining showed that metformin enhanced the expression of Ki-67 in vascular endothelial cells. Furthermore, both immunofluorescence staining and FCM demonstrated that metformin increased Gli1 expression in vascular endothelial cells. Additionally, cell counting Kit-8 (CCK8) and viability assays of HUVECs in vitro both indicated that metformin improved the vascular proliferation and tube formation of HUVECs under 90% oxygen. These results indicated that metformin enhanced lung vascular development and upregulated the expression of Gli1 in the pulmonary vascular endothelial cells in hyperoxic neonatal mice.

Keywords: Bronchopulmonary dysplasia (BPD), hyperoxia, sonic hedgehog signaling (Shh), vascular development, metformin

Introduction

Bronchopulmonary dysplasia (BPD) is the most common and serious chronic lung disease affecting premature infants [1]. There is an intricate pathogenetic mechanism that play in BPD leading to arrested alveolar and vascular lung development [2]. Angiogenesis is necessary for alveolarization during normal lung development [3]. Infants with BPD who died have abnormal alveolar microvessels and disordered expression of angiogenic growth factors [4]. As BPD lacks effective treatment strategies, understanding the mechanism how alveoli and the underlying capillary network develop is disrupted is critical for developing effective therapies for BPD [5].

The Hedgehog (Hh) family of intercellular signaling proteins are key mediators in many fundamental embryonic developmental processes, and are essential in regulating cell differentiation [6]. Sonic Hedgehog (Shh), one of the members of this family, is critical for cell differentiation, and its aberrant expression may result in abnormal lung development [7]. The receptor, Patched-1 (Ptch1), binds to Shh glycoproteins in the presence of the Shh ligand, which abrogates the inhibition of activity of the 7-transmembrane protein Smoothened (SMO) and

induces downstream transcription factor Gli1 to enter the nucleus, thus regulating cell differentiation [8]. Recent studies have shown that Hh signaling is involved in vascular development, and it is possible that the diminished airway branching in Shh-deficient mice is due to abnormal pulmonary vascular formation [9]. The Shh signaling pathway facilitated vascular proliferation in developing embryos, ischemic corneas, and limbs of aged rats; it also promoted angiogenesis in neurogenic tumors [10]. Additionally, Shh pathway activity reduced remarkably in diabetic endothelial progenitor cells (EPCs), and the activation of Shh in Shh-modified diabetic EPCs rescued the myocardial repair of diabetic mice through the Shh/BMI1 proto-oncogene (Bmi1)/p53 axis [11].

Metformin is a biguanide that is widely used to treat patients diagnosed with type II diabetes by enhancing insulin sensitivity, inducing glycolysis, and suppressing glyconeogenesis in the liver [12]. Metformin enhanced angiogenesis by upregulating vascular endothelial growth factor (VEGF) expression and reducing chemokine ligand 10 mRNA, and alleviated diabetic cardiopathy within a hyperglycemia-hypoxia environment [13]. It was reported that metformin enhanced the migration of human umbilical vein endothelial cells (HUVECs) under high glucose concentration and promoted the angiogenic potential of endothelial cells in diabetic foot ulcer by engaging the AMPK signaling pathway [14]. Niu and coworkers found that metformin increased Gli1 expression of the Shh signaling pathway and alleviated the endothelial leakage in response to hyperglycemia-induced endothelial dysfunction [15]. Moreover, metformin enhanced the leakage of vascular endothelial cells and alleviated pulmonary inflammation by upregulating AMPK mRNA in hyperoxic newborn rats [16]. However, whether metformin can enhance vascular development in BPD is unknown. In this study, we investigated the effects of metformin on pulmonary vascular development and the potential role of the Shh signaling pathway in a neonatal BPD mouse model subjected to prolonged hyperoxia.

Materials and methods

Animal care and drug treatment

All experimental procedures were conducted in accordance with the relevant guidelines and regulations of the care and use of animals as defined by the Expert Committee of Laboratory Animal Sciences of the Shanghai Jiao Tong University School of Medicine. Timed-pregnant C57BL/6J mice were provided by the central laboratory animal center of Xinhua Hospital Shanghai Jiao Tong University School of Medicine. The animals were kept indoors at $23\pm2°C$ and subjected to a fluorescent lighting cycle (12-h light-dark cycle, light from 6:00 am to 6:00 pm). Newborn mice within postnatal 12 h were randomly divided into four groups: room air with saline group (RA + saline), room air with metformin group (RA + metformin), 85% oxygen with saline group (HO + saline), 85% oxygen with metformin group (HO + metformin), with 16 mice in each group along with the lactating mothers. For the intervention administration, pups were subcutaneously injected with metformin (100 mg/kg, D150959, Sigma-Aldrich, St. Louis, MO, USA) from the second day onwards after being exposed to a hyperoxic environment; the controls were injected with saline and were subjected to the same procedure. Hyperoxia-exposed pups were raised in a hermetic plexiglass chamber, and the nursing mothers were rotated daily to avoid oxygen toxicity until postnatal day 14 (P14). Oxygen levels were monitored continuously using a Miniox II monitor.

Cell culture and culture conditions

Human umbilical vein endothelial cell (HUVEC) lines were purchased from Cell Bank of Chinese Academy of Sciences (Shanghai, China). The cells were cultured in DMEM supplemented with 10% FBS, 1% penicillin/streptomycin at 37°C in a humidified 5% CO_2 atmosphere. For experiments, the cells were seeded and pre-treated with different concentrations of metformin or PBS as control after the no-adherent cells were removed with PBS. Then the cells were cultured in 90% oxygen or 21% oxygen for 24 h or 48 h. After the treatment, the cells were analyzed as described below.

Viability assay (CCK8)

HUVECs were planted into 96 well plates containing culture medium. Subsequently, HUVECs were treated with different concentration of metformin under 90% oxygen for 48 h. After treatment, viability assays were conducted with the cell counting Kit-8 (CCK8). The density of

the solubilized formazan was read at 450 nm spectrophotometrically (Bio-rad, Hercules, CA).

Tube formation assay

HUVECs were divided into four groups: 21% oxygen with saline group (Control + Saline), 21% oxygen with metformin group (Control + metformin), 90% oxygen with saline group (HO + Saline) and 90% oxygen treated with metformin group (HO + Metformin). One thousand HUVEC were suspended with 20 mM metformin and seeded onto matrigel (356234; Corning, Gorilla, NY) 96 wells plates, followed by the hyperoxia or 21% oxygen. Capillary morphogenesis was examined after 24 h under a phase contrast and fluorescent microscope (B201; Olympus, Tokyo, Japan). The number of branch points per HPF was counted, and the length of capillaries was quantified by Image J.

Morphometric analysis

The mice were anesthetized and sacrificed at postnatal day 7 (P7) or day 14 (P14) of treatment and lungs were harvested for morphometric analysis. Each lung tissue was embedded in paraffin after being fixed with 4% paraformaldehyde, and then stained with hematoxylin and eosin (H&E). Morphometric images were captured under a microscope (B201; Olympus, Tokyo, Japan) at 200× magnification. Three pups were selected from each group, and five random non-overlapping fields in one distal lung section per pup were utilized for morphometric examination. Radial alveolar counts, the terminal airspaces, and secondary septa in each field were manually counted to analyze lung development.

Immunohistochemistry analysis

Immunohistochemistry staining was performed to identify the microvascular density. Immunohistochemistry on paraffin-embedded and sectioned lung samples was performed using a standard procedure. Briefly, slides were deparaffinized and rehydrated. Tissue was then permeabilized and peroxidases were blocked in 0.3% hydrogen peroxide. Slides were incubated with blocking buffer (phosphate buffered solution, 0.1% Triton X-100, 5% goat serum) for 1 h at room temperature and then incubated with primary antibody overnight at 4°C with the following antibodies: anti-

PECAM-1 (CD31) antibody (1:50, Servicebio, Shanghai, China). After washing, slides were exposed to secondary antibody conjunction with HRP (horseradish peroxidase) for 1 h at room temperature, washed again, and then staining was performed using DAB peroxidase substrate kit (Sangon Biotech, Shanghai, China); this was followed by counterstaining with hematoxylin. The images were observed and scanned using Pannoramic MIDI at 400× magnification.

Immunofluorescence staining

The proliferation of vascular endothelial cells was evaluated by immunofluorescence staining. After 14 days of intervention, lungs were harvested and sections were prepared. The CD31 and Ki-67 double positive cells were manually counted. Subsequently, the sections were stained with anti-PECAM-1 (CD31) antibody (1:50, Servicebio, Shanghai, China), anti-Gli1 antibody (1:100, Abcam, Cambridge, MA), anti-Ki67 antibody (1:50, Servicebio, Shanghai, China), and DAPI (1:100, Servicebio, Shanghai, China). Fluorescence microscopy (Pannoramic MIDI, Tokyo, Japan) was used to scan at 400× magnification.

Western blotting assays

Lung tissues were homogenized in lysis buffer (RIPA + PMSF). Samples were sonicated for 16 s, and were then centrifuged at 12500 rpm at 4°C for 25 min. Supernatants were transferred to clean tubes, and total protein was determined by the BCA protein assay (Beyotime Institute of Biotechnology, Shanghai, China).

Equal amounts of protein were electrophoresed in 6% or 12% SDS-polyacrylamide gel and then transferred onto polyvinylidene fluoride membranes. After blocking with 5% non-fat dried milk for 1.5 h at room temperature, the membranes were incubated overnight at 4°C with anti-PECAM-1 (CD31) antibody (1:1000, Servicebio, Shanghai, China) and GAPDH antibody (1:1000, Beyotime Institute of Biotechnology, Shanghai, China) as the loading control. After washing in Tris-buffered saline containing 1% Tween 20, the membrane was incubated with secondary antibody (anti-rabbit IgG horseradish peroxidase conjugate 1:2000; anti-mouse IgG horseradish peroxidase conjugate 1:2000) for 2 h at room temperature. The
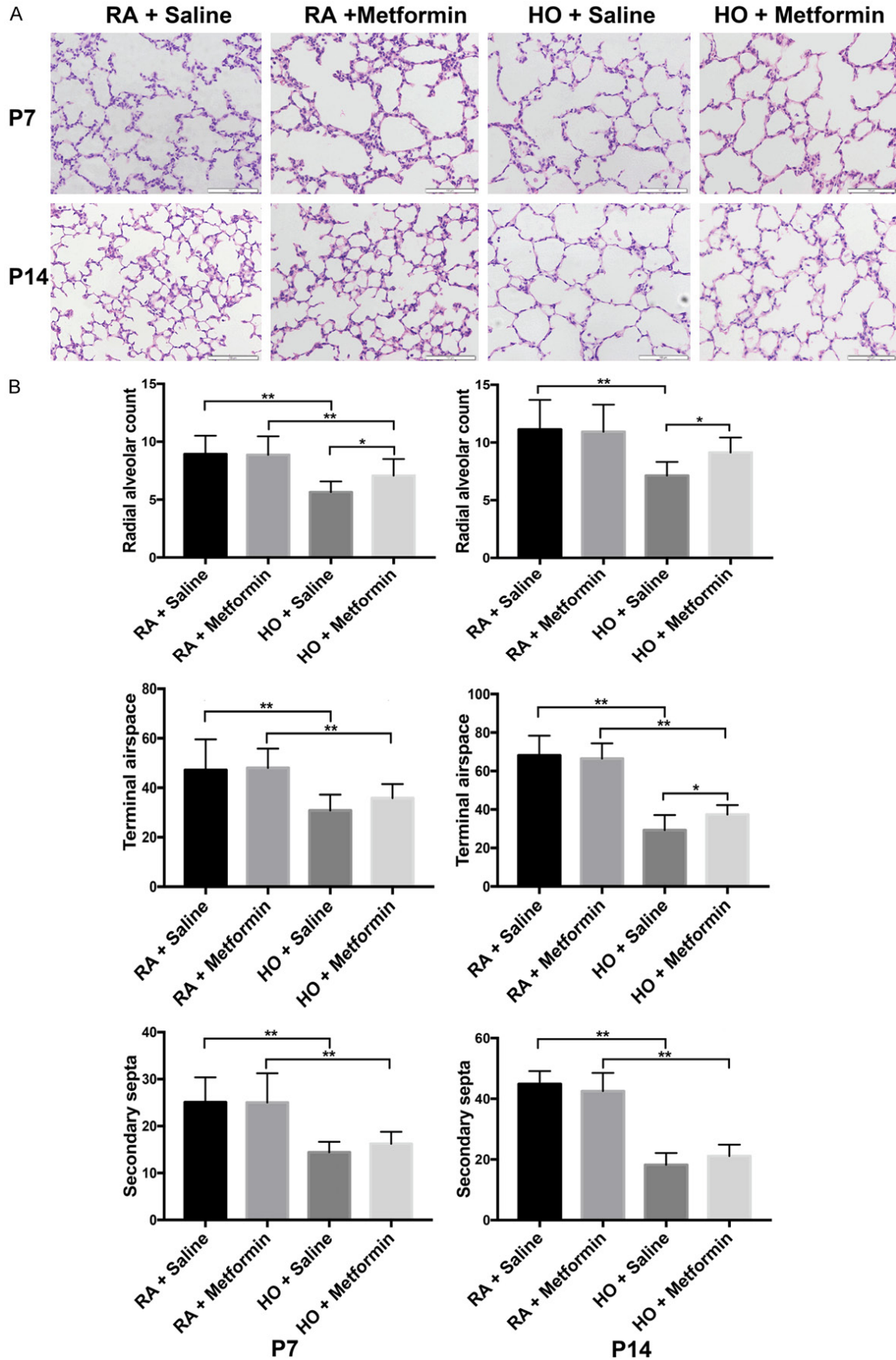
Figure 1. Metformin attenuated lung impairment in hyperoxic lung injury in newborn mice. A. Representative lung morphological sections stained with H&E on P7 and P14; magnification: 200×, scale bar: 100 μm. B. Quantification of radial alveolar count, terminal airspace, and secondary septa. All images were acquired under the same condition and displayed at the same scale (Data represent the mean ± SD. *P<0.05, **P<0.01).
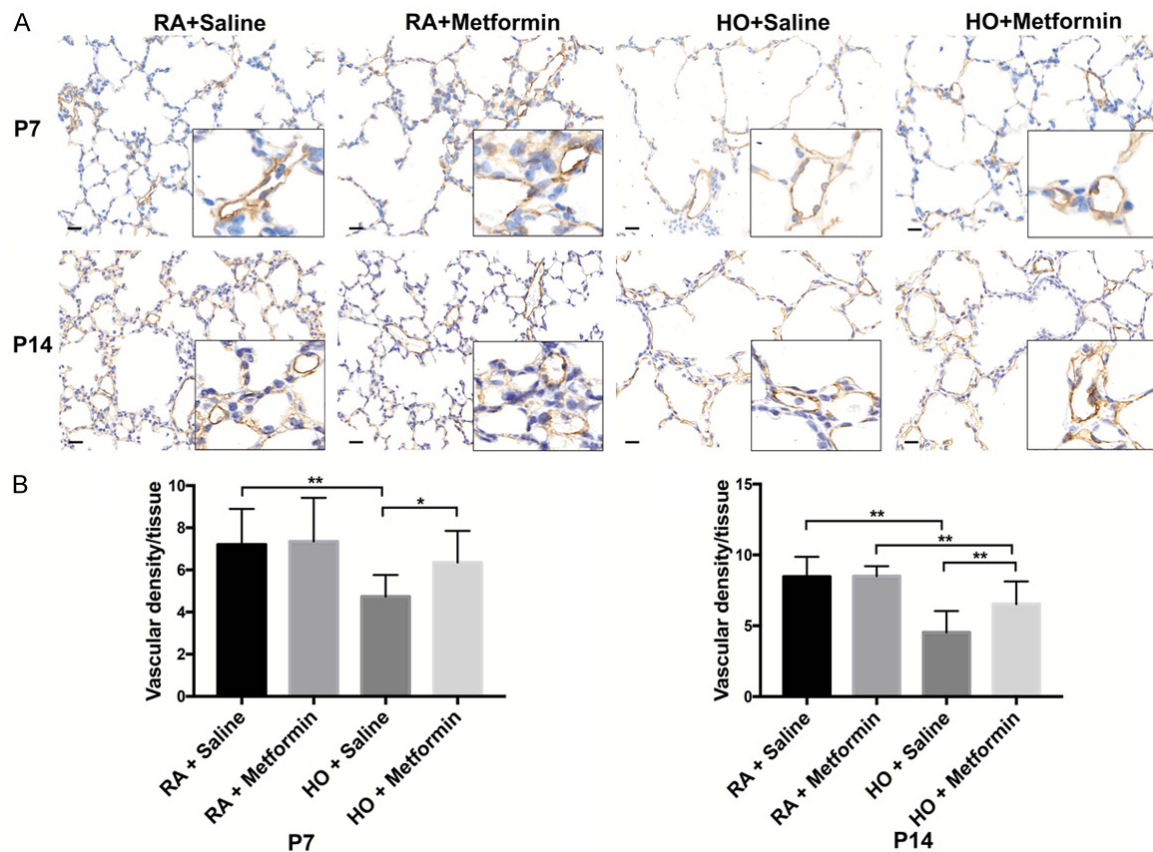

Figure 2. Metformin enhanced the vascular density and the expression of CD31 in hyperoxic lung injury on P7 and P14. A. Immunohistochemistry staining showed that metformin enhanced the vascular density on P7 and P14; B. Quantitative analysis of the percentage of microvascular density by manual counting on P7 and P14. magnification: 400×, scale bar: 20 μm. All images were acquired under the same condition and displayed at the same scale (Data represent the mean ± SD. *P<0.05, **P<0.01).

western blots were detected using electrochemiluminescent reagents (Millipore Corporation, Billerica, MA). Three samples from each group were analyzed.

Flow cytometry

Whole lungs were processed by enzymatic and mechanical digestion to yield a single suspension for flow cytometry (FCM) as described previously [17]. First, the isolated whole lung was put into a culture dish 6 cm in diameter, and washed twice in cold PBS to get rid of the blood. Second, lung tissues were cut into pieces using sharp ophthalmic scissors, then incubated with 5 ml digestion buffer, comprising 2 ml

Collagenase/Dispase (1 mg/ml, Roche Diagnostics, Basel, Swit), 2 ml 0.025% Trypsin (Gibco, Grand Island, NY), 1 ml DNase I (Roche Diagnostics, Basel, Swit) at 37°C for 30 min, and again mechanically disrupted with a 1000-μl pipette Incubation was continued for 20 min. Third, the digestion buffer was passed through a 100-μm cell strainer (BD Falcon, Franklin lakes, NJ) to yield a single suspension and remove connective tissue. Fourth, the filtered buffer was added to 2 ml lysis buffer to eliminate red cells, and centrifuged at 600 relative centrifugal force (rcf, for 5 min at 4°C). Then, the cell pellet was washed in PBS after removing the supernatant and centrifuged as
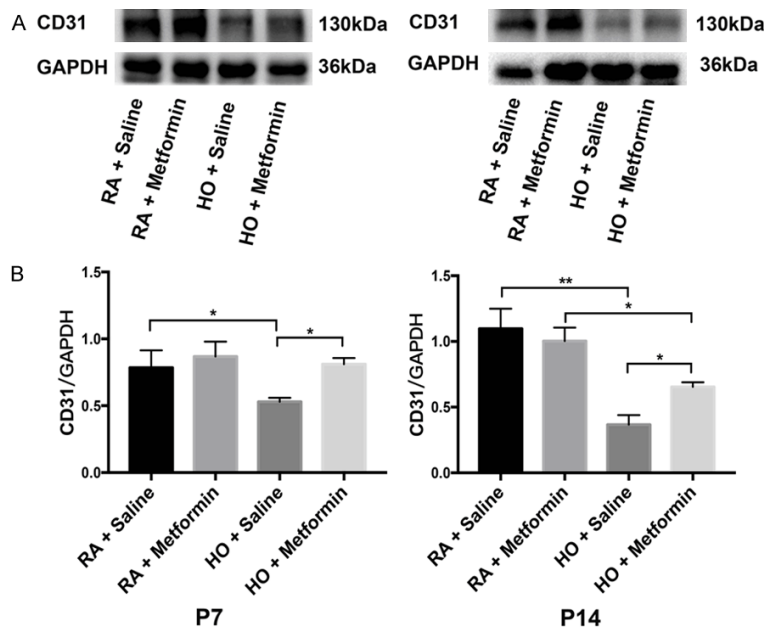
Figure 3. Metformin increased the expression of Pecam-1 (CD31) in the lung of newborn mice exposed to hyperoxia on P7 and P14. A. Western blotting assays showed that metformin significantly upregulated the expression of CD31 in the lung of the hyperoxic mice on P7 and P14. B. Quantitative analysis of the level of CD31 protein by Image J (Data represent the mean ± SD. *$P<0.05$, **$P<0.01$).

heterogeneous distribution of enlarged air spaces with less terminal airspaces ($P<0.01$), reduced radial alveolar counts ($P<0.01$), and less secondary septa ($P<0.01$). Metformin had no effect on lung development in the room air group ($P>0.05$). However, metformin increased the number of terminal airspaces ($P<0.05$) and the radial airspace counts ($P<0.05$) on P14 in the hyperoxia group, with no effect on secondary septa (**Figure 1A**, **1B**). These results suggested that metformin enhanced alveolar development in hyperoxic lung injury.

Metformin enhanced vascular development in hyperoxia-induced lung injury

Immunohistochemistry staining showed that exposure to hyperoxia significantly resulted in decreased lung vascular density in newborn mice ($P<0.01$) and metformin increased the vascular density on P7 and P14 ($P<0.05$) (**Figure 2A**, **2B**). Western blotting assays demonstrated that the expression of CD31 in the lung decreased significantly on P7 and P14 after exposure to hyperoxia ($P<0.01$). Nevertheless, metformin increased the expression of CD31 on P7 and P14 in the hyperoxia group ($P<0.05$) (**Figure 3**).

Additionally, the proliferation of vascular endothelial cells was investigated using immunofluorescence staining with CD31 and Ki-67 (**Figure 4A**). Exposure to hyperoxia resulted in decreased activity of the vascular endothelial cells on P14 compared with the room air group ($P<0.01$). Administration of metformin significantly enhanced the ability of vascular endothelial cells to proliferate after exposure to hyperoxia ($P<0.05$) (**Figure 4B**).

Metformin upregulated the expression of Gli1 in the lung

Immunofluorescence staining showed that Gli1 was present in vascular endothelial cells. The expression of Gli1 in vascular endothelial cells decreased in the hyperoxia group compared
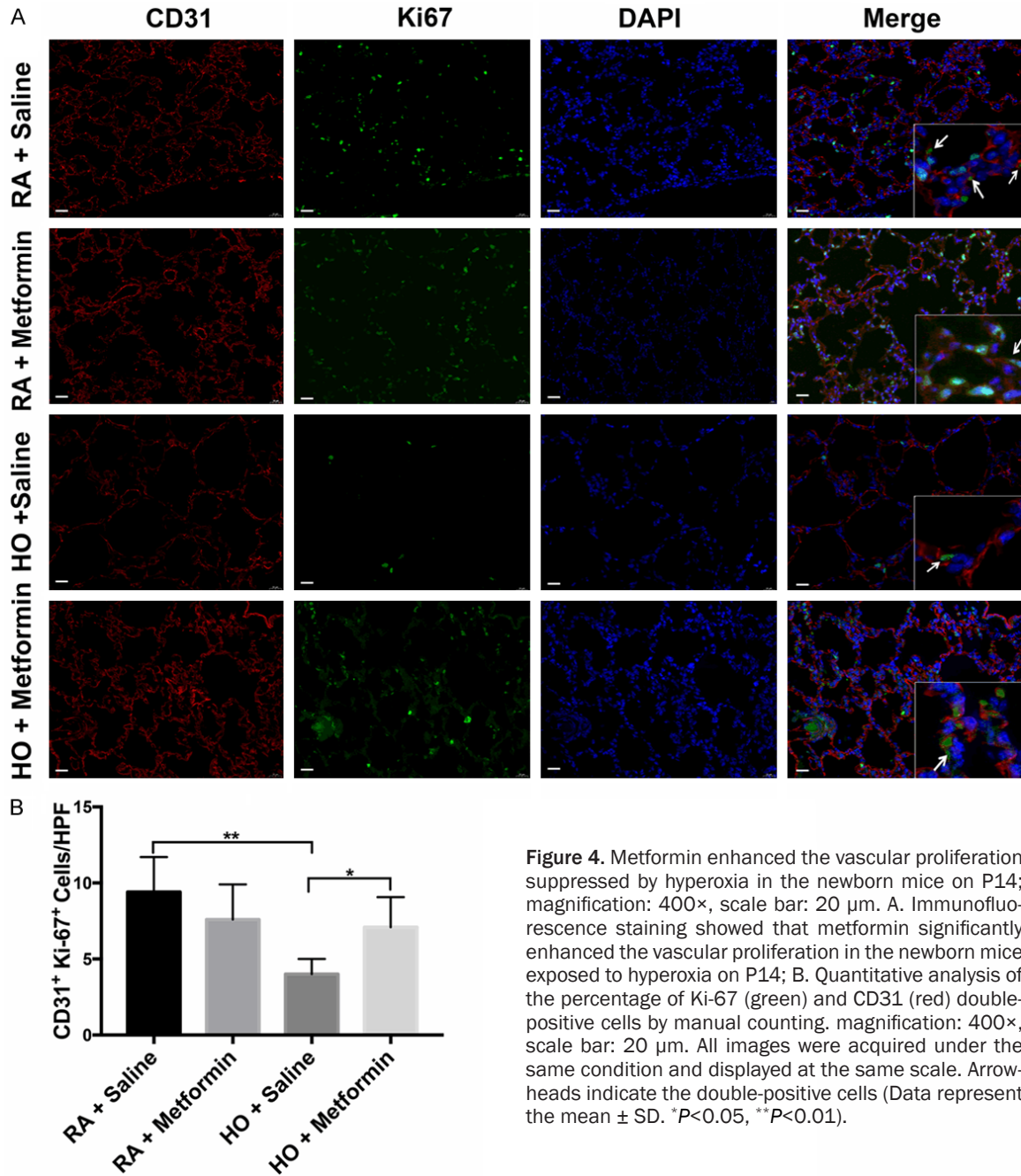
above. Following this, the cell pellet was resuspended in PBS and prepared for FCM. We investigated the relationship between Gli1 and vascular endothelial cells by co-localizing both indicated antibody markers: Gli1 and anti-PECAM-1 (CD31) (Invitrogen, Carlsbad, CA), and CD45 (Invitrogen, Carlsbad, CA) was used to exclude the blood cells. Stained cells were separated using cell sorting (Cytoflex; Beckman Coulter, Fullerton, CA).

Statistical analysis

GraphPad Prism 7.0 software was used for statistical analysis. All results are presented as mean ± SD, and statistical analyses were performed using one-way or two-way ANOVA with Tukey's multiple comparisons test. A *P* value <0.05 was considered statistically significant.

Results

Metformin attenuated hyperoxia-induced lung impairment

Almost all the pups in the room air and hyperoxia groups survived until the end of the animal experiments. Exposure to hyperoxia significantly resulted in impaired lung on P7 and P14, a
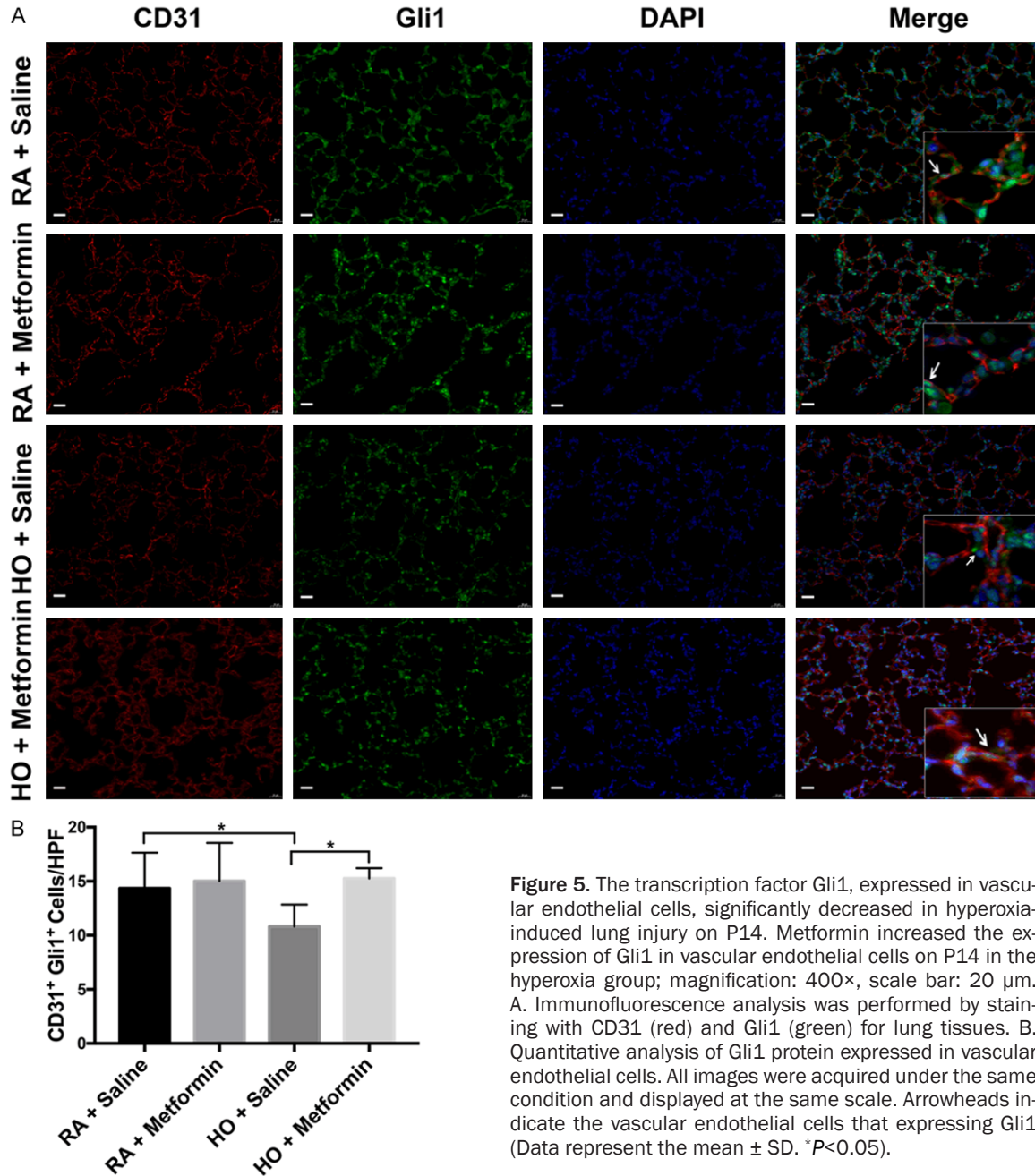
Figure 4. Metformin enhanced the vascular proliferation suppressed by hyperoxia in the newborn mice on P14; magnification: 400×, scale bar: 20 µm. A. Immunofluorescence staining showed that metformin significantly enhanced the vascular proliferation in the newborn mice exposed to hyperoxia on P14; B. Quantitative analysis of the percentage of Ki-67 (green) and CD31 (red) double-positive cells by manual counting. magnification: 400×, scale bar: 20 µm. All images were acquired under the same condition and displayed at the same scale. Arrowheads indicate the double-positive cells (Data represent the mean ± SD. $^*P<0.05$, $^{**}P<0.01$).

with that in the room air group ($P<0.05$) (**Figure 5A, 5B**). However, metformin enhanced Gli1 expression in vascular endothelial cells ($P<0.05$) (**Figure 5A, 5B**). These results indicated that Gli1 might play a vital role in hyperoxic lung injury in neonatal mice.

Furthermore, FCM was used to investigate the expression of Gli1 in vascular endothelial cells (**Figure 6A**). Blood cells were first excluded using CD45 staining, and CD31$^+$ cells repre-

sented vascular endothelial cells. Expression of Gli1 decreased in vascular endothelial cells on P14 in the hyperoxia group compared with that in the room air group (P<0.01). Metformin increased the expression of Gli1 in vascular endothelial cells on P14 in the hyperoxia group (P<0.05) (**Figure 6B**). These results suggested that metformin may upregulate the expression of Gli1 in endothelial cells and promote pulmonary vascular development.

Figure 5. The transcription factor Gli1, expressed in vascular endothelial cells, significantly decreased in hyperoxia-induced lung injury on P14. Metformin increased the expression of Gli1 in vascular endothelial cells on P14 in the hyperoxia group; magnification: 400×, scale bar: 20 μm. A. Immunofluorescence analysis was performed by staining with CD31 (red) and Gli1 (green) for lung tissues. B. Quantitative analysis of Gli1 protein expressed in vascular endothelial cells. All images were acquired under the same condition and displayed at the same scale. Arrowheads indicate the vascular endothelial cells that expressing Gli1 (Data represent the mean ± SD. *P<0.05).

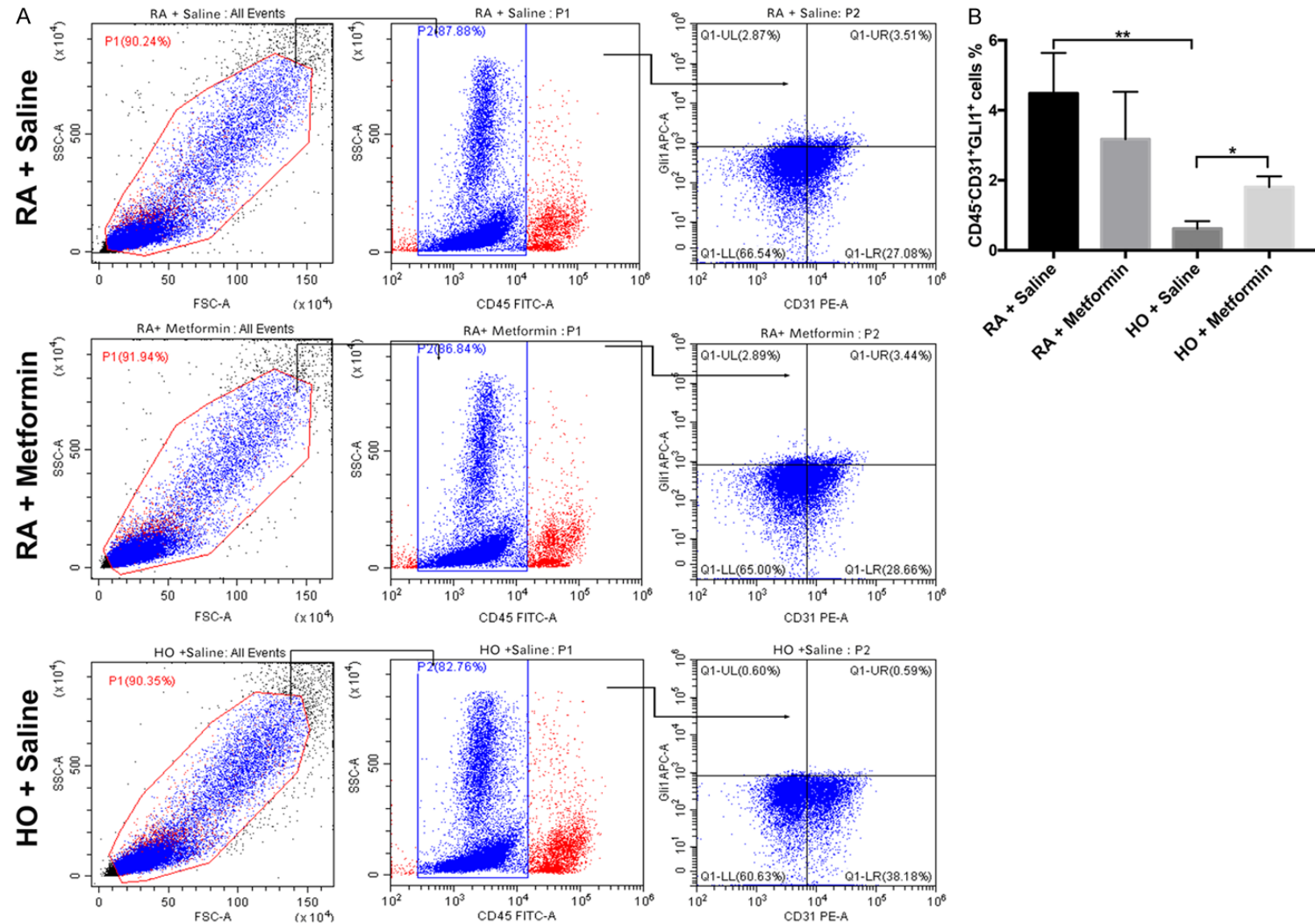*Metformin improved the viability and tube formation of HUVECs*

The cell counting Kit-8 assays indicated that 90% oxygen significantly inhibited the proliferation of HUVECs (P<0.01) comparing with control group, and metformin at 20 mM improved the cellular proliferation and survival exposed to 90% oxygen (P<0.01) (**Figure 7**). Moreover, the improvement of metformin in HUVECs had an obvious dose effect. Furthermore, the tube formation assays also showed that exposure to hyperoxia resulted in the decreased number of tube than control group (P<0.01), however, metformin (20 mM) enhanced the tube formation of HUVECs exposed to 90% oxygen (P<0.01) (**Figure 8**). These results also indicated that metformin had a potential role in vascular development under hyperoxia in vitro.

Discussion

Our data indicated that metformin enhanced pulmonary vascular development and the expression of Gli1 in vascular endothelial cells
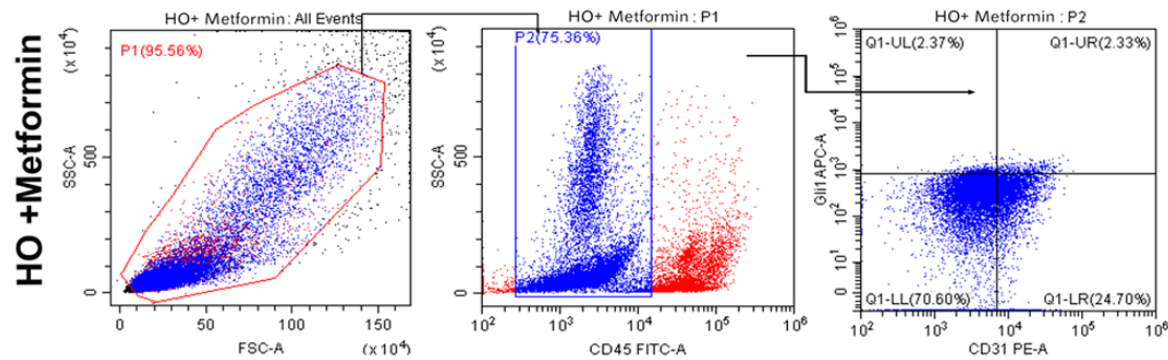
Figure 6. Metformin enhanced the expression of Gli1 in vascular endothelial cells in hyperoxia-induced lung injury. There are at least three mice from each group. Single-cell preparations of lungs from each group were subjected to FACS. A. Metformin upregulated the level of Gli1 in vascular endothelial cells in the lung of newborn mice exposed to hyperoxia. B. Quantitative analysis of the percentage of the vascular endothelial cells that expressing Gli1. Immune cells were screened by staining with CD45 (Data represent the mean ± SD. $^{*}P<0.05$, $^{**}P<0.01$).
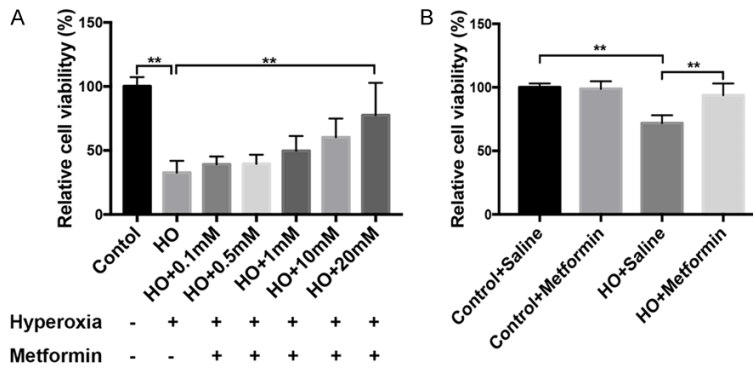
Figure 7. Metformin improved the vascular proliferation of HUVECs exposed to 90% oxygen for 48 h in vitro. A. The effects of metformin on HUVECs had a time-dose dependence. B. Metformin at 20 mM significantly promoted the proliferation and survival of HUVECs in vitro under hyperoxia (Data represent the mean ± SD. **$P<0.01$).

in hyperoxic lung injury in newborn mice. It was reported that metformin significantly enhanced the expression of transcription factor Gli1 to downregulate autophagy-induced endothelial cell death [15]. The Shh signaling pathway may process angiogenesis via upregulation of VEGF, Angiopoietin-1 (Ang-1), and Angiopoietin-2 (Ang-2) to induce vascular proliferation in ischemia-reperfusion injury [18].

Infants dying from BPD showed disrupted pulmonary vascular development with decreased angiogenesis-related factors, including VEGF, vascular endothelial growth factor receptor-1 (Flt-1), and tyrosine kinase receptor (Tie-2) [19]. In the present study, the pathological consequences included arrested alveolar structure and vascular development in the lungs of hyperoxia-exposed mice. Pulmonary vasculature development comprises of two basic processes, namely vasculogenesis and angiogenesis [20]. During angiogenesis, complex structures, beginning with the pre-existing vessels and union of the peripheral sinusoids, follow the path of branching airways in order to develop [4]. Cumulative studies have suggested that extensive microvascular network not only effectively promoted normal alveolar development but also contributed to the maintenance of alveolar structures [4, 21].

Members of the Hedgehog family of intercellular signaling proteins were recognized as pivotal mediators of embryonic development in the 1990s [6]. The Hh signaling pathway mediates the formation of woven bone and angiogenesis

in postnatal osteogenesis by regulating HIF-α levels during stress fracture healing [22]. The Sonic hedgehog signaling pathway is indispensable in embryonic lung morphogenesis [23]. Cumulative studies identified that Shh promoted the differentiation of nerves and pulmonary vasculature during the embryonic period [24]. Gli1 is a transcription factor, whose overexpression in the lung mesenchyme promotes Ptch1 gene expression in lung development [23]. It was found that Shh signaling was involved in organizing specified angioblasts into vascular tubes, and Shh was the first growth factor identified to regulate vascular tube formation [25]. In recent years, Kramann and co-workers. discovered that Gli1-positive perivascular cells in the outermost vessel layer were progenitors, initiating pathological vessel remodeling [26]. In this study, we found that Gli1 was localized in CD31^{+} vascular endothelial cells, and decreased significantly in response to hyperoxia. Even though the Shh signaling pathway has been linked to angiogenesis by various lines of investigation, the underlying mechanism is unclear, and some studies indicated that Shh acted directly on endothelial cells [27-29]. Micro-RNA-153 (miR-153) has protective effects on ischemic injury; the upregulation of miR-153 activated the Shh signaling pathway to promote angiogenesis in middle cerebral artery occlusion [30]. The Shh signaling pathway upregulated F-actin formation through Shh/Gli1/integrin β1 and downregulated E-cadherin expression through the Shh/matrix metalloproteinase (MMP) 2/9 signaling pathway to promote angiogenesis in a wound repair mouse model [31, 32]. Administration of the Shh hedgehog pathway agonist (SAG) rescued neurological deficit and enhanced angiogenesis, through promoting neuron regeneration and reducing cellular apoptosis in a mouse model with brain ischemia [33]. In addition, increasing evidence demonstrated that the Shh signaling pathway may play a role in tumor development by promoting angiogenesis in various tumors [34, 35]. Application of SAG actively promoted vascular proliferation and
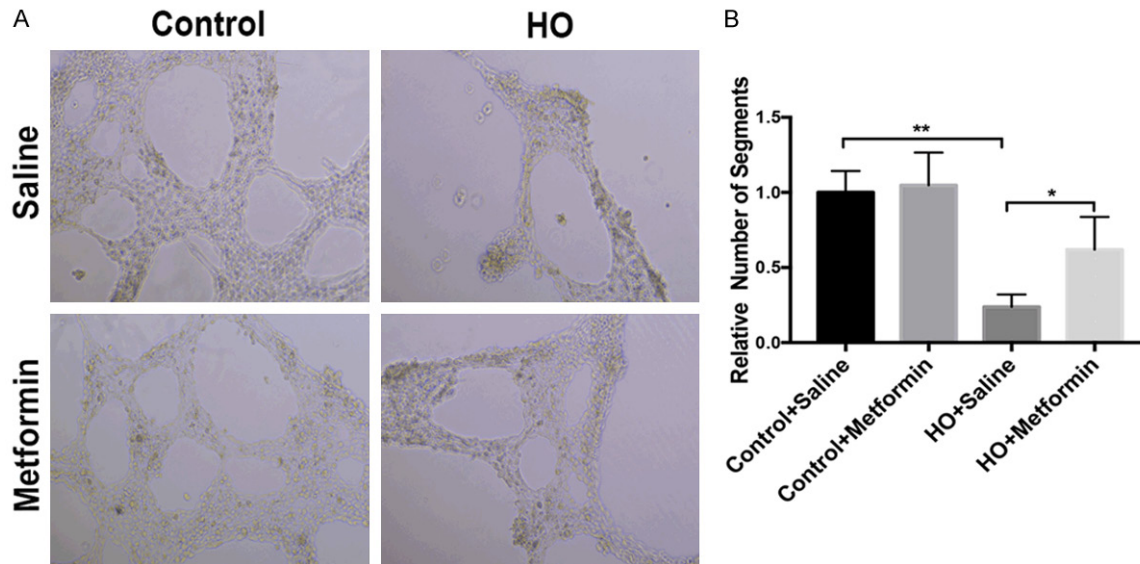
Figure 8. Metformin promoted the tube formation of HUVECs exposed to hyperoxia. A. Metformin enhanced differentiation into tubular network structure under 90% oxygen for 24 h in vitro. B. Quantitative analysis of tubular network formation under the different experimental conditions expressed as network projections per low-power field (Data represent the mean ± SD. **$P<0.01$).

enhanced the reperfusion volume through upregulating VEGF expression in the brain ischemic area; however, the inhibitor of Shh reversed the positive effects [36]. In the present study, we also found that Shh signaling pathway was involved in vascular development in hyperoxia-induced lung injury.

Metformin is one of the primary oral first-line drugs for the treatment of type II diabetes due to its ability to increase insulin sensitivity and decrease glycose uptake. Metformin has also been used in the treatment of other diseases, as is evidenced by cumulative research in recent years [37]. Metformin reduced inflammation by activating the AMPK pathway and improved ischemia-induced brain atrophy by facilitating the proliferation of CD31^{+} vascular endothelial cells [38]. Metformin promoted endothelial precursor cells (EPCs) in accelerating angiogenesis by increasing the intracellular nitric oxide (NO) level in a diabetic mouse model with wound healing impairments [39]. Pre-treatment of diabetic patients with metformin was found to be associated with reduced myocardial infarction size [40]. The cardioprotection mechanism of metformin was unclear. Metformin restored the VEGFA pathway through upregulating VEGFR1/2, leading to a dual effect on the activation of cell migration through MMP16 and ROCK1 upregulation, in addition to inhibition of apoptosis by increase

in phospho-ERK1/2 and FABP4 [41]. Moreover, metformin was used to rescue limb ischemia, enhancing the blood flow volume and upregulating VEGF to increase the vascular density in a mouse model [42]. In our study, metformin significantly improved the vascular proliferation in vivo and vitro under hyperoxia and upregulated the expression of Gli1 in vascular endothelial cells in the hyperoxic mice. Additionally, metformin induced VEGF protein, augmented the CD31^{+} and CD34^{+} cells, and inhibited the apoptosis of vascular endothelial cells in wound areas [43]. Another study found that metformin upregulated Ras guanine-releasing protein 1 (RasGRP1) dependent VEGF signaling and restored impaired angiogenesis in diabetic models [44].

In conclusion, metformin was found to enhance lung vascular development and proliferation of vascular endothelial cells in neonatal mice exposed to hyperoxia. In addition, metformin upregulated the expression of Gli1 in pulmonary vascular endothelial cells in hyperoxic BPD mice. The detailed mechanism of metformin action on the Shh signaling pathway and its effect on vascular development in BPD should be investigated further.

Acknowledgements

Disclosure of conflict of interest

None.

Address correspondence to: Hongping Xia, Department of Neonatology, Xinhua Hospital, Shanghai Jiao Tong University School of Medicine, 1665 Kongjiang Road, Shanghai 200092, China. Tel: +86-21-2507-8320; Fax: +86-21-6503-0840; E-mail: xiahongping@xinhuamed.com.cn

References

[1] Alvira CM and Morty RE. Can we understand the pathobiology of bronchopulmonary dysplasia? J Pediatr 2017; 190: 27-37.

[2] Jobe AH. The new bronchopulmonary dysplasia. Curr Opin Pediatr 2011; 23: 167-172.

[3] Jakkula M, Cras TDL, Gebb S, Hirth KP, Tuder RM, Voelkel NF and Abman SH. Inhibition of angiogenesis decreases alveolarization in the developing rat lung. Am J Physiol Lung Cell Mol Physiol 2000; 279: L600-L607.

[4] Bhatt AJ, Pryhuber GS, Huyck H, Watkins RH, Metlay LA and Maniscalco WM. Disrupted pulmonary vasculature and decreased vascular endothelial growth factor, Flt-1, and Tie-2 in human infants dying with bronchopulmonary dysplasia. Am J Respir Crit Care Med 2001; 164: 1971-1980.

[5] Thébaud B and Abman SH. Bronchopulmonary dysplasia: where have all the vessels gone? Roles of angiogenic growth factors in chronic lung disease. Am J Respir Crit Care Med 2007; 175: 978-985.

[6] Ingham PW and McMahon AP. Hedgehog signaling in animal development: paradigms and principles. Gene Dev 2001; 15: 3059-3087.

[7] Lim S, Lim SM, Kim MJ, Park SY and Kim JH. Sonic hedgehog pathway as the prognostic marker in patients with extensive stage small cell lung cancer. Yonsei Med J 2019; 60: 898-904.

[8] Rimkus TK, Carpenter RL, Qasem S, Chan M and Lo HW. Targeting the Sonic hedgehog signaling pathway: review of Smoothened and Gli inhibitors. Cancers (Basel) 2016; 8: 22-44.

[9] Van Tuyl M, Groenman F, Wang J, Kuliszewski M, Liu J, Tibboel D and Post M. Angiogenic factors stimulate tubular branching morphogenesis of sonic hedgehog-deficient lungs. Dev Biol 2007; 303: 514-526.

[10] Alfaro AC, Roberts B, Kwong L, Bijlsma MF and Roelink H. Ptch2 mediates the Shh response in Ptch1-/- cells. Development 2014; 141: 3331-3339.

[11] Xiao Q, Zhao XY, Jiang RC, Chen XH, Zhu X, Chen KF, Chen SY, Zhang XL, Qin Y, Liu YH and Luo JD. Increased expression of sonic hedgehog restores diabetic endothelial progenitor cells and improves cardiac repair after acute myocardial infarction in diabetic mice. Int J Mol Med 2019; 44: 1091-1105.

[12] Martin-Montalvo A, Mercken EM, Mitchell SJ, Palacios HH, Mote PL, Scheibye-Knudsen M, Gomes AP, Ward TM, Minor RK, Blouin MJ, Schwab M, Pollak M, Zhang Y, Yu Y, Becker KG, Bohr VA, Ingram DK, Sinclair DA, Wolf NS, Spindler SR, Bernier M and De Cabo R. Metformin improves healthspan and lifespan in mice. Nat Commun 2013; 4: 2192.

[13] Bakhashab S, Ahmed FW, Schulten HJ, Bashir A, Karim S, Al-Malki AL, Gari MA, Abuzenadah AM, Chaudhary AG, Alqahtani MH, Lary S, Ahmed F and Weaver JU. Metformin improves the angiogenic potential of human CD34+ cells co-incident with downregulating CXCL10 and TIMP1 gene expression and increasing VEGFA under hyperglycemia and hypoxia within a therapeutic window for myocardial infarction. Cardiovasc Diabetol 2016; 15: 27-38.

[14] Zolali E, Rezabakhsh A, Nabat E, Jaberi H, Rahbarghazi R and Garjani A. Metformin effect on endocan biogenesis in human endothelial cells under diabetic condition. Arch Med Res 2019; 50: 304-314.

[15] Niu C, Chen Z, Kim KT, Sun J, Xue M, Chen G, Li S, Shen Y, Zhu Z, Wang X, Liang J, Jiang C, Cong W, Jin L and Li X. Metformin alleviates hyperglycemia-induced endothelial impairment by downregulating autophagy via the hedgehog pathway. Autophagy 2019; 15: 843-870.

[16] Chen X, Walther FJ, Sengers RM, Laghmani el H, Salam A, Folkerts G, Pera T and Wagenaar GT. Metformin attenuates hyperoxia-induced lung injury in neonatal rats by reducing the inflammatory response. Am J Pysiol Lung Cell Mol Physiol 2015; 309: L262-L270.

[17] Xia H, Ren X, Bolte CS, Ustiyan V, Zhang Y, Shah TA, Kalin TV, Whitsett JA and Kalinchenko VV. Foxm1 regulates resolution of hyperoxic lung injury in newborns. Am J Resp Cell Mol 2015; 52: 611-621.

[18] Guo W, Yi X, Ren F, Liu L, Wu S and Yang J. Activation of Shh signaling pathway promotes vasculogenesis in post-myocardial ischemic-reperfusion injury. Int J Clin Exp Pathol 2015; 8: 12464-12472.

[19] Zhang X, Lu A, Li Z, Sun J, Dai D and Qian L. Exosomes secreted by endothelial progenitor cells improve the bioactivity of pulmonary microvascular endothelial cells exposed to hyperoxia in vitro. Ann Transl Med 2019; 7: 254.

[20] Parera MC, Van Dooren M, van Kempen M, De Krijger R, Grosveld F, Tibboel D and Rottier R. Distal angiogenesis: a new concept for lung vascular morphogenesis. Am J Physiol Lung Cell Mol Physiol 2005; 288: L141-L149.

[21] KasaharaY, Tuder RM, Taraseviciene-Stewart L, Le Cras TD, Abman S, Hirth PK, Waltenberger J and Voelkel NF. Inhibition of VEGF receptors causes lung cell apoptosis and emphysema. J Clin Invest 2000; 106: 1311-1319.

[22] Kazmers NH, Mckenzie JA, Shen TS, Long F and Silva MJ. Hedgehog signaling mediates woven bone formation and vascularization during stress fracture healing. Bone 2015; 81: 524-532.

[23] Liu L, Kugler MC, Loomis CA, Samdani R, Zhao Z, Chen GJ, Brandt JP, Brownell I, Joyner AL, Rom WN and Munger JS. Hedgehog signaling in neonatal and adult lung. Am J Resp Cell Mol Biol 2013; 48: 703-710.

[24] Kusano KF, Pola R, Murayama T, Curry C, Kawamoto A, Iwakura A, Shintani S, Ii M, Asai J, Tkebuchava T, Thorne T, Takenaka H, Aikawa R, Goukassian D, Von Samson P, Hamada H, Yoon YS, Silver M, Eaton E, Ma H, Heyd L, Kearney M, Munger W, Porter JA, Kishore R and Losordo DW. Sonic hedgehog myocardial gene therapy: tissue repair through transient reconstitution of embryonic signaling. Nat Med 2005; 11: 1197-1204.

[25] Voke SA, Yatskievych TA, Heimark RL, McMahon AP, Antin PB and Krieg PA. Hedgehog signaling is essential for endothelial tube formation during vasculogenesis. Development 2004; 131: 4371-4380.

[26] Kramann R, Schneider RK, DiRocco DP, Machado F, Fleig S, Bondzie PA, Henderson JM, Ebert BL and Humphreys BD. Perivascular Gli1+ progenitors are key contributors to injury-induced organ fibrosis. Cell Stem Cell 2015; 16: 51-66.

[27] Alvarez JI, Dodelet-Devillers A, Kebir H, Ifergan I, Fabre PJ, Terouz S, Sabbagh M, Wosik K, Bourbonniere L, Bernard M, Van Horssen J, De Vries HE, Charron F and Prat A. The hedgehog pathway promotes blood-brain barrier integrity and CNS immune quiescence. Science 2011; 334: 1727-1731.

[28] Renault MA, Roncalli J, Tongers J, Thorne T, Klyachko E, Misener S, Volpert OV, Mehta S, Burg A, Luedemann C, Qin G, Kishore R and Losordo DW. Sonic hedgehog induces angiogenesis via Rho kinase-dependent signaling in endothelial cells. J Mol Cell Cardiol 2010; 49: 490-498.

[29] Everson JL, Fink DM, Chung HM, Sun MR and Lipinski RJ. Identification of sonic hedgehog-regulated genes and biological processes in the cranial neural crest mesenchyme by comparative transcriptomics. BMC Genomics 2018; 19: 497.

[30] Wang BX, Xu JJ, Hu J, Hu ML, Huang JM and Zhu XD. Effects of miR-153 on angiogenesis in MCAO rats through Shh signaling pathway. Eur Rev Med Pharmacol Sci 2019; 23: 732-739.

[31] Scully KM, Skowronska-Krawczyk D, Krawczyk M, Merkurjev D, Taylor H, Livolsi A, Tollkuhn J, Stan RV and Rosenfeld MG. Epithelial cell integrin β1 is required for developmental angiogenesis in the pituitary gland. Pron Natl Acad Sci U S A 2016; 113: 13408-13413.

[32] Oh JY, Suh HN, Choi GE, Lee HJ, Jung YH, Ko SH, Kim JS, Chae CW, Lee CK and Han HJ. Modulation of sonic hedgehog-induced mouse embryonic stem cell behaviours through E-cadherin expression and integrin β1-dependent F-actin formation. Br J Pharmacol 2018; 175: 3548-3562.

[33] Jin Y, Barnett A, Zhang Y, Yu X and Luo Y. Poststroke Sonic hedgehog agonist treatment improves functional recovery by enhancing neurogenesis and angiogenesis. Stroke 2017; 48: 1636-1645.

[34] Feng X, Yao J, Gao X, Jing Y, Kang T, Jiang D, Jiang T, Feng J, Zhu Q, Jiang X and Chen J. Multi-targeting peptide-functionalized nanoparticles recognized vasculogenic mimicry, tumor neovasculature and glioma cells for enhanced anti-glioma therapy. ACS Appl Mater Interfaces 2015; 7: 27885-27899.

[35] Takabatake K, Shimo T, Murakami J, Anqi C, Kawai H, Yoshida S, Wathone Oo M, Haruka O, Sukegawa S, Tsujigiwa H, Nakano K and Nagatsuka H. The role of Sonic hedgehog signaling in the tumor microenvironment of oral squamous cell carcinoma. Int J Mol Sci 2019; 20: 5779.

[36] Peng L, Yin J, Ge M, Wang S, Xie L, Li Y, Si JQ and Ma K. Isoflurane post-conditioning ameliorates cerebral ischemia/reperfusion injury by enhancing angiogenesis through activating the Shh/Gli signaling pathway in rats. Front Neurosci 2019; 13: 321-332.

[37] McCreight LJ, Bailey CJ and Pearson ER. Metformin and the gastrointestinal tract. Diabetologia 2016; 59: 426-435.

[38] Liu Y, Tang G, Zhang Z, Wang Y and Yang GY. Metformin promotes focal angiogenesis and neurogenesis in mice following middle cerebral artery occlusion. Neurosci Lett 2014; 579: 46-51.

[39] Han X, Tao Y, Deng Y, Yu J, Sun Y and Jiang G. Metformin accelerates wound healing in type 2 diabetic db/db mice. Mol Med Rep 2017; 16: 8691-8698.

[40] Lexis CP, Wieringa WG, Hiemstra B, Van Deursen VM, Lipsic E, Van der Harst P, Van Veldhuisen DJ and Van der Horst IC. Chronic

metformin treatment is associated with reduced myocardial infarct size in diabetic patients with ST-segment elevation myocardial infarction. Cardiovasc Drugs Ther 2014; 28: 163-171.

[41] Bakhashab S, Ahmed F, Schulten HJ, Ahmed FW, Glanville M, Al-Qahtani MH and Weaver JU. Proangiogenic effect of metformin in endothelial cells is via upregulation of VEGFR1/2 and their signaling under hyperglycemia-hypoxia. Int J Mol Sci 2018; 19: 293-310.

[42] Goggi JL, Haslop A, Boominathan R, Chan K, Soh V, Cheng P, Robins EG and Bhakoo KK. Imaging the proangiogenic effects of cardiovascular drugs in a diabetic model of limb ischemia. Contrast Media Mol Imaging 2019; 2019: 2538909.

[43] Wu H, Ding J, Li S, Lin J, Jiang R, Lin C, Dai L, Xie C, Lin D, Xu H, Gao W and Zhou K. Metformin promotes the survival of random-pattern skin flaps by inducing autophagy via the AMPK-mTOR-TFEB signaling pathway. Int J Biol Sci 2019; 15: 325-340.

[44] Xu J, Liu M, Yu M, Shen J, Zhou J, Hu J, Zhou Y and Zhang W. RasGRP1 is a target for VEGF to induce angiogenesis and involved in the endothelial-protective effects of metformin under high glucose in HUVECs. IUBMB Life 2019; 71: 1391-1400.